D0Note #3201

DRAFT V0.1

Analysis of Events with Large H_T using the Run 1B Data Set

Jay A. Wightman

Iowa State University

Henryk Piekarz

Florida State University

Fred Borcherding

Fermilab

March 27, 1997

Abstract

We have measured the H_T distribution for the Run 1b data set, where H_T is defined as the scalar sum of the E_T of all the jets in the event above a threshold of 20 GeV. This is compared to the distribution generated JETRAD to assess QCD and the Standard Model. This test of QCD is complementary to the inclusive jet analysis as well as the di–jet angular distribution measurements. We find no large disagreement between the data and the predictions of QCD, but we do find room for improvement in our understanding of both the data and the theory.

1 Introduction

It is important to test the limits of QCD both as a means of refining the theory as well as exploring the question of new physics. The usual test that is applied is to study the inclusive jet p_T spectrum and look for deviations from the predictions of either LO or NLO QCD.[1, 2] These tests presuppose a topology where the final–state is principally comprised of two jets resulting from the two final–state partons of the basic $2 \to 2$ process. LO QCD calculations produce such a final state, and higher order calculations are necessary to study the contributions of gluon radiation from the final–state partons.

1.1 Why H_T?

An alternative test of the limits of QCD and, hence, of the Standard Model is to use the total transverse energy released in the interaction. This is a particularly attractive approach as it is independent of the event topology. We found early in Run 1a that it was necessary to use

$$H_T \equiv \sum_{i=1}^{N} E_T^i,$$

where $N =$ the number of jets in the event and E_T^i is the transverse energy of the jet.[3] Scalar E_T is a very efficient trigger for multiple interaction events since it only requires energy deposition in the calorimeter. By switching to H_T we make the concession to an all–jets final state as explained in the offline analysis section. We test QCD through a shape comparison between the H_T distributions of the Run 1b data sample and the Monte Carlo. Doing a shape comparison is one of the strengths of this analysis since it minimizes many of the systematic errors that need to be addressed in an absolute cross section measurement, such as the luminosity and the choice of parton distribution functions and renormalization scale provided that these uncertainties are not E_T–dependent.

While H_T compromises the topology–independence of using Scalar E_T, it makes this analysis complementary to the inclusive jet and di–jet angular distribution analyses. It not only provides an independent test of QCD and the Standard Model, but it also provides a strong consistency check when combined with these other analyses. In addition, H_T is in some sense the most inclusive variable we have in these events. The single biggest problem that the theorists face in trying to understand the experimental data is the definition of a jet and how to convert from partons to jets. The procedure has an inherent difficulty due to the fact that it produces a divergence in the limit $E_T \to 0$. H_T does not suffer from this difficulty since in this limit we can easily add 0 to H_T without causing any problems. Another nice feature of H_T is that there is no problem with splitting and merging of jets provided the jet energy corrections are well-behaved and do not vary rapidly as a function of E_T of the jet.

1.2 Quark Compositeness

Having motivated H_T as a useful variable, we describe a search for quark compositeness. The idea that quarks are composite has more historical prejudice than theoretical. Perhaps the biggest reason for this is because composite quarks are not consistent with a simple extension of the underlying symmetry. With no elegant theory, the theorists are forced to use ad hoc models and so progress in this area is naturally slow.

The model for quark compositeness that we use is described in [4]. There are 12 possible terms in the Lagrangian for composite quarks, but the model simplifies this to use only the left–left isoscalar term (the simplest one). All quarks are assumed to be composite, not just the light quarks; this is the symmetric model. With the simplification to a single, additional term in the Lagrangian, the specification for the model reduces to two parameters, the scale of the interaction (Λ) and the sign of the interference term in the Lagrangian. We examine both signs of this term, constructive and destructive interference, and set limits for each, separately.

2 Data Sample

The data sample for this analysis used the JET_MULTI Level 1 trigger and SCALAR_ET_JT Level 2 trigger which are summarized in Table 1; we refer to this sample as the Large H_T sample. The JET_MULTI Level 1 trigger was not completely stable over the span of Run 1b; it started as 3 large tiles with $E_T > 15$ until the ever–increasing instantaneous luminosity delivered by the Tevatron forced some concessions to be made. The trigger was limited to $|\eta| \leq 2.4$ with requirements on additional trigger towers with $|\eta| \leq 2.6$. The final requirements are shown in Table 1. As discussed in the Offline Analysis section the trigger efficiency for events with $H_T \geq 400$ GeV was unaffected by these machinations. The source of trigger inefficiency was the initial requirement of 3 large tiles since this configuration is not 100% efficient for di–jet events. In addition, the trigger used MAX_LIVE and is susceptible to events due to Main Ring activity.

The SCALAR_ET_JT Level 2 trigger required $E_{Total} \leq 1800$ to discriminate against multiple interaction events. This had the very pleasant feature of roughly maintaining linearity of the trigger rate as a function of the instantaneous luminosity. However, it left us with the unique problem of accounting for the effect of this cut as discussed in the Offline Analysis section.

The luminosity for this trigger is approximately 90.4 pb^{-1}. Through the use of the Run 1b Multiple Interaction Tool[6] this can be sub–divided into probable single interaction events (Tool = 1 or 2) with an integrated luminosity of about 18.1 pb^{-1} and probable multiple interaction events (Tool ≥ 3) which account for approximately 72.3 pb^{-1}.

We have available a second data sample which used an entirely different trigger, the JETMAX sample. The trigger conditions for this trigger are summarized in Table 2. There is about 85–90% overlap between these two samples, consistent with the trigger and blanking conditions. Since the JETMAX sample does not use a cut on E_{Total}, this provides a gauge of how well we understand the Large H_T trigger. We prefer to use the Large H_T sample for our analysis since it does not require at least one very stiff jet.

3 Offline Analysis

3.1 OMNI_FILTER

The Large H_T sample provided two virtual streams from OMNI_FILTER, the NP_SCALAR and NP_SCALAR_TIGHT streams. These filters applied cuts to reconstructed quantities, so the thresholds were allowed to be a little different from the trigger thresholds. The NP_SCALAR filter applied the trigger cut on E_{Total} but reduced the threshold on $\sum |E_T|$ in the calorimeter to 300 GeV. The NP_SCALAR_TIGHT stream also repeated the cut on

E_{Total} but increased the threshold on $\sum |E_T|$ in calorimeter to 370 GeV; it also applied the QCD Bad Jet Finder[7] to the Nearest–Neighbor jets in the event failing the event if any jet failed. This requirement is summarized in Table 3.

3.2 Corrections to the Data

3.2.1 Trigger Efficiency

The trigger efficiency is determined from Monte Carlo hard–scattering events overlayed with non–zero–suppressed ZERO_BIAS events taken in dedicated runs near the end of Run 1b. These data are divided into 5 bins based on the initial instantaneous luminosity of the run as shown in Table 4.

For the MC hard–scattering event sample we used a set of events generated with HERWIG[8] using the CTEQ2L[11] structure function set. To get roughly equal statistics across the spectrum we generate in 7 consecutive, non–overlapping bins of p_T of the leading final–state parton, see Table 5.

For each luminosity bin, one event from the ZERO_BIAS file was overlayed on a non–zero–suppressed event from the Monte Carlo file, the event was zero–suppressed, and the jets were reconstructed. These events were input to the trigger simulator with the full Level 1 and Level 2 trigger requirements applied. A sixth luminosity point (Luminosity = 0) for the trigger efficiency was analyzed without overlaying any ZERO_BIAS events. The trigger efficiency for all 6 luminosity bins is shown in Fig. 1.

The fits to the points in Fig. 1 are with the error function convoluted with a gaussian to smear the rising edge and multiplied by a linear function to provide the downward slope of the trigger efficiency for $H_T \geq 400$ GeV for the non–zero luminosity bins. The character of the trigger efficiency noted in Fig. 1 can be easily understood as the combination of the Level 2 trigger conditions with the multiple interaction environment of Run 1. The turn–on of the trigger is due to the threshold on $\sum |E_T|$ in the calorimeter; the fact that the efficiency never reaches 1.0 results from the Level 1 requirement of 3 large tiles which is not fully efficient for di–jet events. In the Monte Carlo, events with larger H_T also tend to have larger E_{Total}, as well. Since multiple interactions add to E_{Total}, it is easy to see that the trigger efficiency decreases with increasing H_T due to the cut on E_{Total}. Since this efficiency depends on H_T and the luminosity, it is applied on an event–by–event basis.

One consequence of increasing instantaneous luminosity and, thus, increasing multiple interactions on the trigger efficiency of the Large H_T sample is to move the rising edge to lower values of H_T. Therefore, we look to the zero luminosity distribution to set the minimum value of H_T for our data. In addition, we apply the $+1\sigma$ high fluctuation in the jet energy scale to make sure that we avoid the rising edge of this distribution. The results are shown in the upper plot in Fig. 2 where we show the trigger turn on curve for both the nominal and high jet energy scale. We also include two vertical lines at $H_T = 450$ and 500 GeV as a guide to the eye to show the range over which the minimum H_T could possibly vary; we set $H_T^{min} = 500$ GeV. In the two lower plots of Fig. 2 we include the trigger turn on curves for both the JETMAX and JET85 event samples. These are found directly from the data. We include vertical lines in each plot as a guide to the eye in showing H_T^{min} for each of these two jet triggers.

3.2.2 QCD Bad Jet Finder

The QCD Bad Jet Finder is described in detail in [7]. The efficiency of this cut is parameterized as a function of the E_T of the jet for cone 0.7 jets as

$$(0.978 - 0.00019 \times E_T)$$

Since H_T is a scalar sum of the E_T of each jet above the threshold of 20 GeV, the efficiency of this cut for each event is a product of the efficiency for each jet in the event. Therefore, this efficiency is also applied on an event–by–event basis.

3.2.3 Hot Cells

During Runs 1b–c the Level 2 processor farm ran the AIDA Hot Cell Killer to search each event for anomalously large calorimeter energy deposits and flag these cells as suspected Hot Cells. In the event reconstruction, these flagged cells were not included in the jet finding procedure or in the determination of the $\not{E}_T$. Careful study by the Inclusive Jet group of these Hot Cells in the vicinity of a jet finds that for many jets there is no justification of removing these cells. They suggest the following procedure for studying these cells. The cell is added into the nearest jet within the radius of the jet cone by recomputing first the centroid of the jet and then its $E_T, \eta,$ and ϕ.

This updated jet is required to pass the QCD Bad Jet Finder. If it passes, then the $\not\!\!E_T$is also recomputed for the addition of the cell. We follow this same procedure for the Large H_T sample, except that if any updated jet fails the Bad Jet Finder requirements then we fail the entire event (like in OMNI_FILTER).

3.2.4 Primary Vertex Check

Large H_T events can be mimicked by lower H_T events if the primary scattering vertex is mis–identified. Again, we follow the procedure developed by the QCD group for choosing the primary vertex if more than one is identified in an event. We take advantage of the fact that we are studying hadronic QCD events and, thus, expect no $\not\!\!E_T$ from the interaction; the $\not\!\!E_T$ we expect to measure will generally be due to mismeasurement of one or more jets in the event. In Monte Carlo events without multiple interactions, there is a strong correlation between $\not\!\!E_T$ and $\not\!\!H_T$, missing H_T calculated from the vector sum of the E_T of the jets. Inclusion of multiple interactions decreases this correlation, but the fact remains that for correct identification of the primary vertex $\not\!\!H_T$ will be a minimum. Therefore, for each vertex identified in the event, we recompute the E_T of each jet and $\not\!\!H_T$; the vertex which minimizes $\not\!\!H_T$ is selected as the primary vertex, and H_T is calculated with respect to it.

3.2.5 $\not\!\!E_T$

The Inclusive Jet group has developed a form of $\not\!\!E_T$–significance cut to remove residual cosmic rays, main ring activity, and spurious energy fluctuations from the data set. They require the ratio between $\not\!\!E_T$ and the leading jet E_T to be less than 0.7. Most of these effects result in a single, high–E_T jet. For the Large H_T sample the trigger has effectively removed these anomalous events so that this cut is not required here. By requiring 3 Large Tiles at Level 1 and placing an upper limit on $E_{T_{otal}}$ at Level 2, we remove these offending events. All that remains are a small handful of events all of which have $H_T \leq 500$ GeV.

4 Monte Carlo

We use 3 different Monte Carlo event generators for this analysis. We use PYTHIA[9] to generate the non–SM physics processes, HERWIG[8] to provide the trigger efficiency, and JETRAD[10] to generate the SM distribution for comparison with the data. For each Monte Carlo H_T distribution we fit a smoothing function. This way we can compare to the data and have any fluctuations be due only to the data. The smoothing function we fit is one we call a cubic exponential,

$$e^{a+b\times H_T+c\times H_T^2+d\times H_T^3}.$$

The fit is done using MINUIT with each of the four coefficients, $a-d$, allowed to vary.

4.1 PYTHIA

PYTHIA is a leading–order generator that is very versatile due to the large number of input parameters. An example of this versatility is the relatively large number of non–SM processes that have been included in the event generation. To minimize systematic uncertainties between the different generators we want to generate SM and non–SM with the same generator. In this way systematic effects should cancel in the comparison. At the very least we can determine a K–factor from PYTHIA which is the ratio of non–SM to SM. Of the three event generators we have used, PYTHIA is the only one to provide non–SM processes, so the K–factor is necessary to simulate non–SM in the other generators, see Figs. 3–6.

We modified the TEST release version of PYTHIA to generate weighted events with the weighting function

$$\left(\frac{p_T}{650}\right)^{10},$$

where p_T is the leading parton p_T in GeV/c. This flattened the cross section as a function of H_T to a distribution that varied by less than one order of magnitude. For each run we generated 2×10^6 events in the range, 50 GeV/c $\leq p_T \leq$ 650 GeV/c. An example of one such distribution along with the fit to a cubic exponential is shown in Fig. 7a. In Fig. 7b we show the raw spectrum overlayed on the weighted spectrum from which the cross section is calculated.

4.2 HERWIG

HERWIG is also a leading–order generator, but it does the best job of the leading–order generators in reproducing measured jet variables. The events we generated with HERWIG have used the multiple p_T bin prescription described above and have been used to study the trigger efficiency, see Fig. 1 and Table 5. For the trigger efficiency we need to use DØGEANT, DØRECO, and TRIGSIM, and it is not possible to do this with the multi–million event samples.

4.3 JETRAD

JETRAD is a next–to–leading–order generator that is used for almost all QCD analyses whenever possible. JETRAD generates weighted events as the default, and for each of our runs we generate 88×10^6 events. An example of one such run with the fit to the cubic exponential smoothing function is shown in Fig. 7c.

4.4 Options

The biggest question to answer regarding Monte Carlo events after choice of generator is the choice of parton distribution functions and renormalization scale. In theory this should not matter as all of these calculations must converge to describing the same physics; however, in practice, this is not the case. An example of this dependence is shown in Fig. 8 where we take ratios between the smoothing functions. In Fig. 8a–b we use the CTEQ2ML structure functions to study the renormalization scales, $\mu = 0.5, 1.0,$ and $1.5 \times E_T$ of the leading jet. In Fig. 8c–f we set $\mu = 0.5 \times E_T$ and study differences between the CTEQ2ML, MRSD-[12], CTEQ3L, and CTEQ3M structure functions.

5 Results

In this section we discuss how the Monte Carlo H_T distributions compare with the Run 1b data sample and the limit on the scale of quark compositeness. To make the comparison we normalize the Monte Carlo distribution to match the data in the bin $H_T = 500$ GeV (centered at $H_T = 512.5$ GeV) thus eliminating the dependence on the luminosity. Since it is difficult to see small differences between distributions on a log plot, we use (Data − Theory)/Theory to show any differences on a linear scale.

5.1 Systematic Errors

As we discussed in Section 1, our comparison between data and Monte Carlo involves normalizing the Monte Carlo distribution to match the data in a single bin of H_T. This eliminates some systematic uncertainties, like the integrated luminosity, from the problem and greatly reduces others due to the bin–to–bin correlations, like the jet energy scale uncertainty. The trigger efficiency also contributes to the overall systematic uncertainty but only negligibly. This is due once again to the normalization that we do.

The largest systematic error is then that due to the jet energy scale determination. To estimate this error, we allow the jet energy scale to fluctuate to its $\pm 1\sigma$ limits to produce the limits on the H_T distribution in the data. We normalize these distributions in the same manner as the nominal jet energy scale distribution and take the ratio between the limit and the nominal distributions. We approximate the bin–to–bin ratio as a linear function in H_T.

5.2 Data Checks

In this section we describe various checks we have applied to our analysis to make sure that we have not introduced any anomalous behavior in the method. For all of our comparisons discussed in the next section we use as our standard Monte Carlo distribution the JETRAD sample with the CTEQ3M parton distributions and $\mu = 0.5 \times E_T$ of the leading jet. In all comparisons the error bars shown on the data points are statistical from the data added in quadrature with the fully correlated errors on the Monte Carlo smoothing function.

5.2.1 Multiple vs. Single Interactions

As noted above, we have chosen to use the full event sample and not restrict our analysis to single interaction events. The comparison of the full Large H_T sample with the Monte Carlo is shown in Fig. 9a where we include the systematic errors due to the jet energy scale. Since multiple interactions comprise approximately 80% of our data sample, as determined by the Run 1b Multiple Interaction Tool[6], it behooves us to verify our original assumption that H_T is robust in the multiple interaction environment of Run 1. In Fig. 9b we show the comparisons of those events flagged as probable single interactions with the JETRAD distribution, and in Fig. 9c we do the same for those events flagged as probable multiple interactions. Within the limited statistics of the single interaction event sample (accounts for only about 20% of the data sample), it is seen that the two distributions (SI and MI) are consistent with each other and with the full data sample.

5.2.2 Comparison with the JETMAX sample.

As discussed earlier, we can compare with the independently triggered JETMAX sample. In Fig. 9d we show the comparison between the H_T distribution from the JETMAX event sample and the JETRAD Monte Carlo distribution. Again, this distribution compares favorably with that of Fig. 9a, so that we can conclude that these two samples yield consistent results.

5.3 Comparison between Theory and Data

For our comparison between theory and data we use for our theory the JETRAD generated event sample with the CTEQ3M parton distribution functions and a renormalization scale, $\mu = 0.5 \times E_T$ of the leading jet. To simulate the non–SM physics of composite quarks, we apply the K–factors shown in Figs. 3–6 to the JETRAD SM distribution. We plot (Data − Theory)/Theory to make the comparison on a linear scale as shown in Figs. 10–13. For each comparison we include the systematic error band due to the jet energy scale uncertainty. The error bars on the points are the statistical errors in the data combined in quadrature with the fully correlated errors from the fit of the smoothing function. The Monte Carlo distribution that best describes the data will produce a flat distribution; it will be centered on 0 on the vertical scale by virtue of the fact that we normalize each Monte Carlo cross section to match the data in the first bin.

As can be seen in Figs. 10–13, the Run 1b data are not best described by the Standard Model. There are several possible explanations for this that do not involve invoking new physics. The Run 1b jet energy scale has still not been finalized, both in terms of the nominal energy scale and the errors. In addition, the deviation we note between the SM and the data may be signalling a deficiency in our understanding of the theory.

6 Conclusions

We have measured the H_T distribution for the Run 1b data sample with $H_T \geq 500$ GeV. Comparing this with the H_T distribution from QCD as given by the JETRAD Monte Carlo event generator we find reasonably good agreement, but it is by no means perfect. With several questions still open, like the final determination of the jet energy scale with its errors, we do not address the question of extensions to the Standard Model.

Despite years of work on QCD and the Standard Model, we still have not nailed it down completely. The theorists are always looking for new ways to view the problem, and the measurements we describe in this note represent a novel approach to understanding hard–scattering events.

References

[1] DØ Run 1b inclusive jet analysis DØ note and PRL in preparation.

[2] F. Abe, et al., *Phys. Rev. Lett.* **77**, 438 (1996).

[3] "Analysis of Events with Large Total Transverse Energy," Henryk Piekarz and Jay Wightman, DØnote 2315, unpublished.

[4] E. Eichten, I. Hinchliffe, K. Lane, and C. Quigg, *Rev. Mod. Phys.* **56**, 579 (1984) and references therein.

[5] "Determination of the Hadronic Energy Scale of DØ Calorimetry (CAFIX version 5.0)," B. Kehoe and R. Astur, DØnote 2908, unpublished.

[6] "Multiple Interaction Tool Study for Run 1," W. Carvalho and T. Taylor, DØnote 2798, unpublished.

[7] QCD Jet Users Guide.

[8] G. Marchesini, B.R. Webber, G. Abbiendi, I.G. Knowles, M.H. Seymour, and L. Stanco, *Computer Physics Commun.* **67**, 465 (1992).

[9] H.–U. Bengtsson and T. Sjöstrand, *Computer Physics Commun.* **46**, 43 (1987). We use PYTHIA V5.7.

[10] W. Giele, E. Glover, and D. Kosower, *Nucl. Phys.* **B403**, 633 (1993).

[11] CTEQ Series 2: J. Botts, et al., *Phys. Lett.* **304B**, 159 (1993); CTEQ Series 3: MSUHEP–41024.

[12] A.D. Martin, R.C. Roberts, and W.J. Stirling, *Phys. Rev.* **D47**, 867 (1993).

Table 1: Run 1b Trigger Conditions – Large H_T sample.

Trigger	Conditions
L1: JET_MULTI	3 Large Tiles ($E_T \geq 15$ GeV and $\vert\eta\vert \leq 2.4$) + 3 Jet Towers ($E_T \geq 7$ GeV and $\vert\eta\vert \leq 2.6$) + MAX_LIVE
L2: SCALAR_ET_JT	Scalar_ET $\geq$ 375 GeV + $E_{Total} \leq 1800$ GeV

Table 2: Run 1b Trigger Conditions – JETMAX sample.

Trigger	Conditions
L1: JET_MAX	1 Large Tile ($E_T \geq 45$ GeV) + 2 Large Tiles ($E_T \geq 10$ GeV) + GOOD_CAL
L2: JET_MAX	1 Jet ($E_T \geq 115$ GeV)

Table 3: QCD Bad Jet Requirements

Condition	Cut
CH Fraction	≤ 0.40
EM Fraction	≥ 0.05 and ≤ 0.90 ≤ 0.90 only if jet in ICR
Hot Cell Ratio (Ratio highest E_T cell to second highest)	≤ 10.0

Table 4: Non–Zero–Suppressed ZERO_BIAS Runs

Run Number	Luminosity ($\times 10^{30}$)	Number of Events
92248	3.29	7017
91911	5.35	5086
92129	10.0	3613
92668	13.8	3366
92685	19.2	1460

Table 5: HERWIG event samples for Trigger Study

p_T bin (GeV/c)	Number of Events
120–200	1933
200–280	1926
280–360	1925
360–440	1951
440–520	1961
520–600	1963
600–640	1974

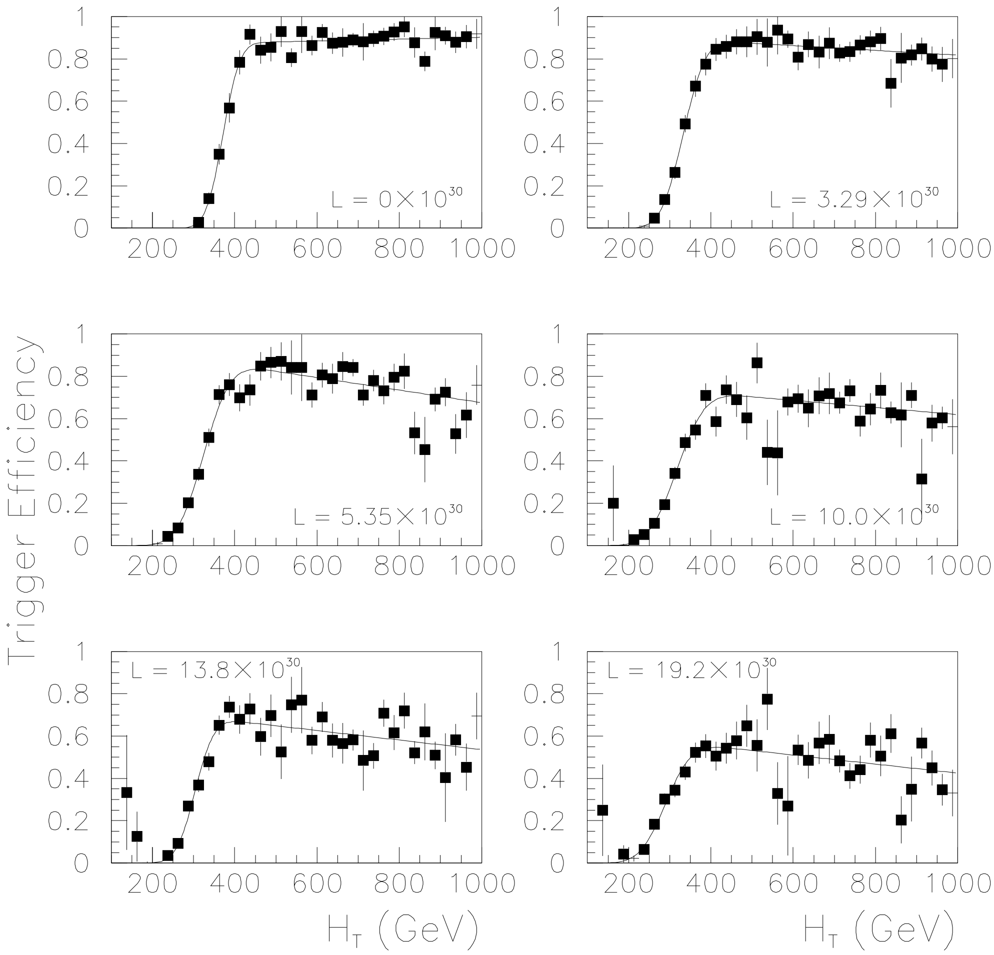

Figure 1: Trigger efficiency as a function of luminosity bin.

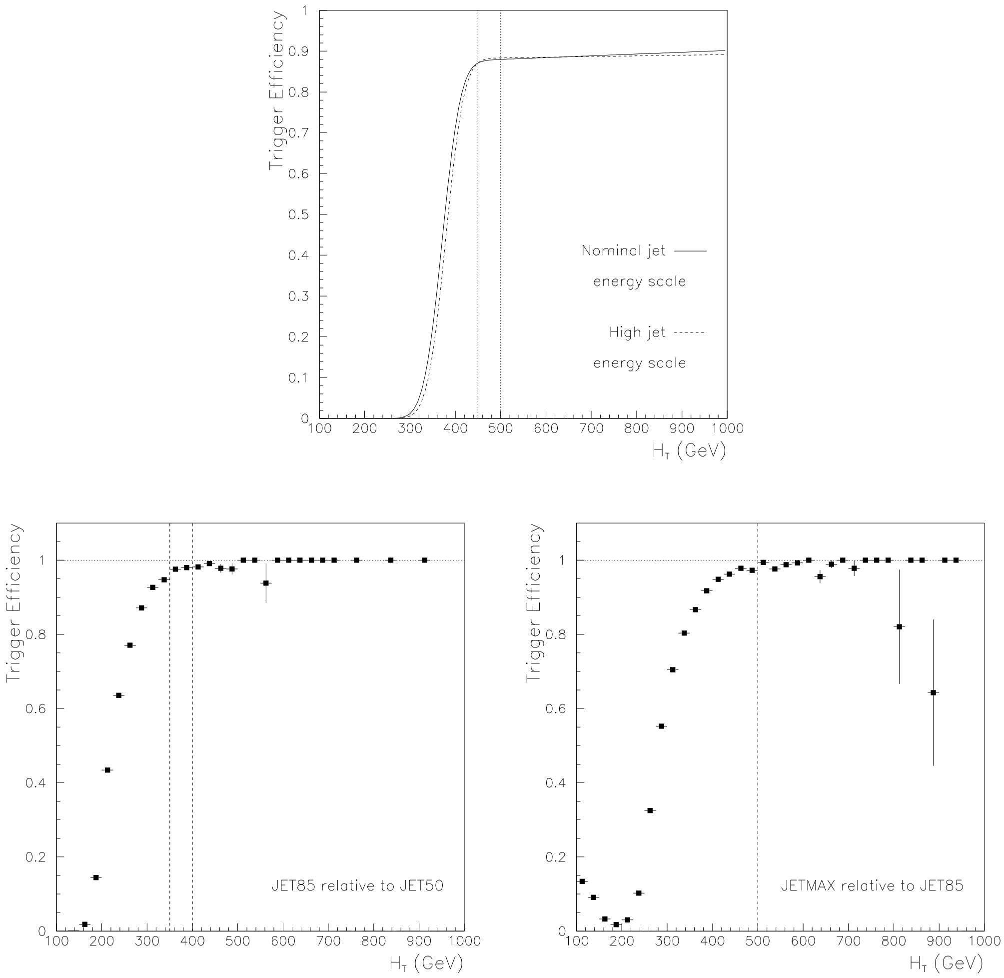

Figure 2: Trigger turn on curves for the Large H_T sample (upper plot) and the two highest E_T jet triggers in the lower plots.

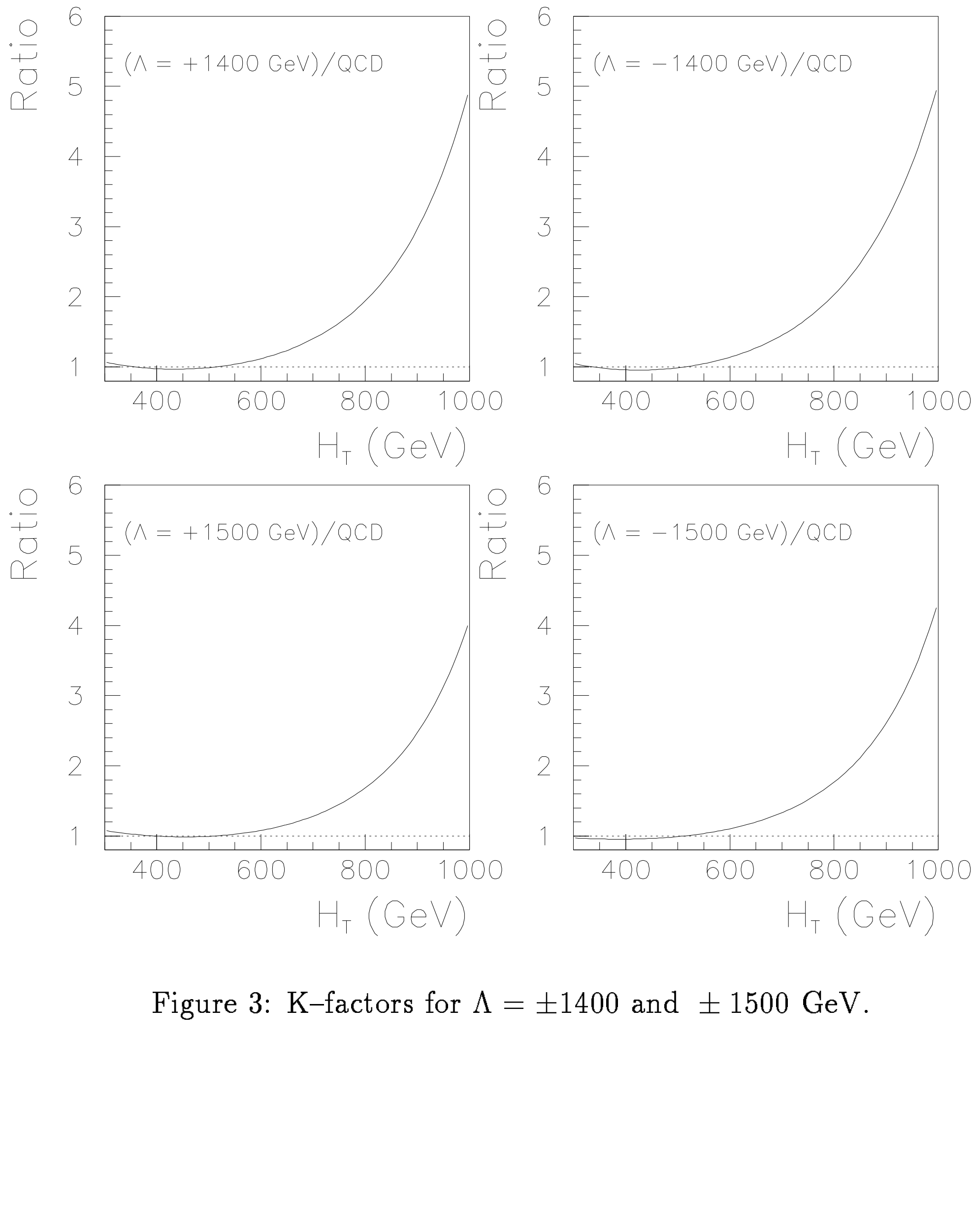

Figure 3: K–factors for $\Lambda = \pm 1400$ and ± 1500 GeV.

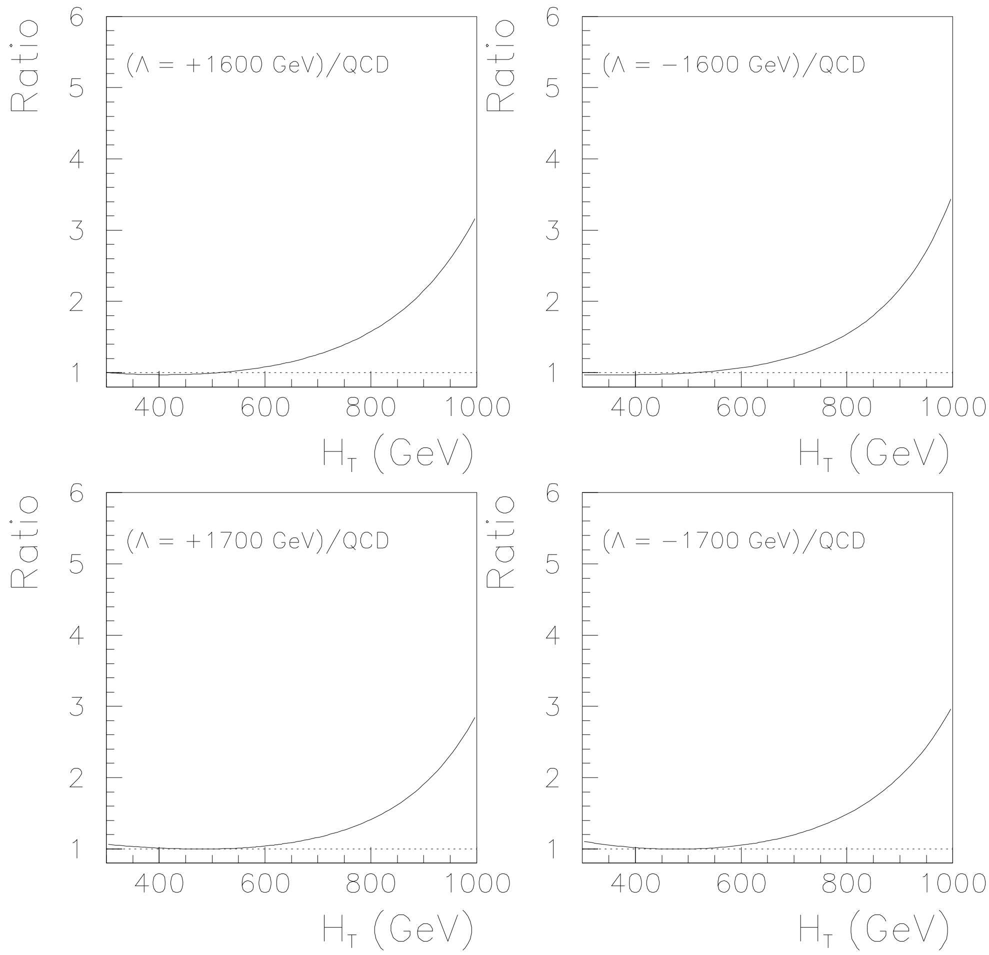

Figure 4: K–factors for $\Lambda = \pm 1600$ and ± 1700 GeV.

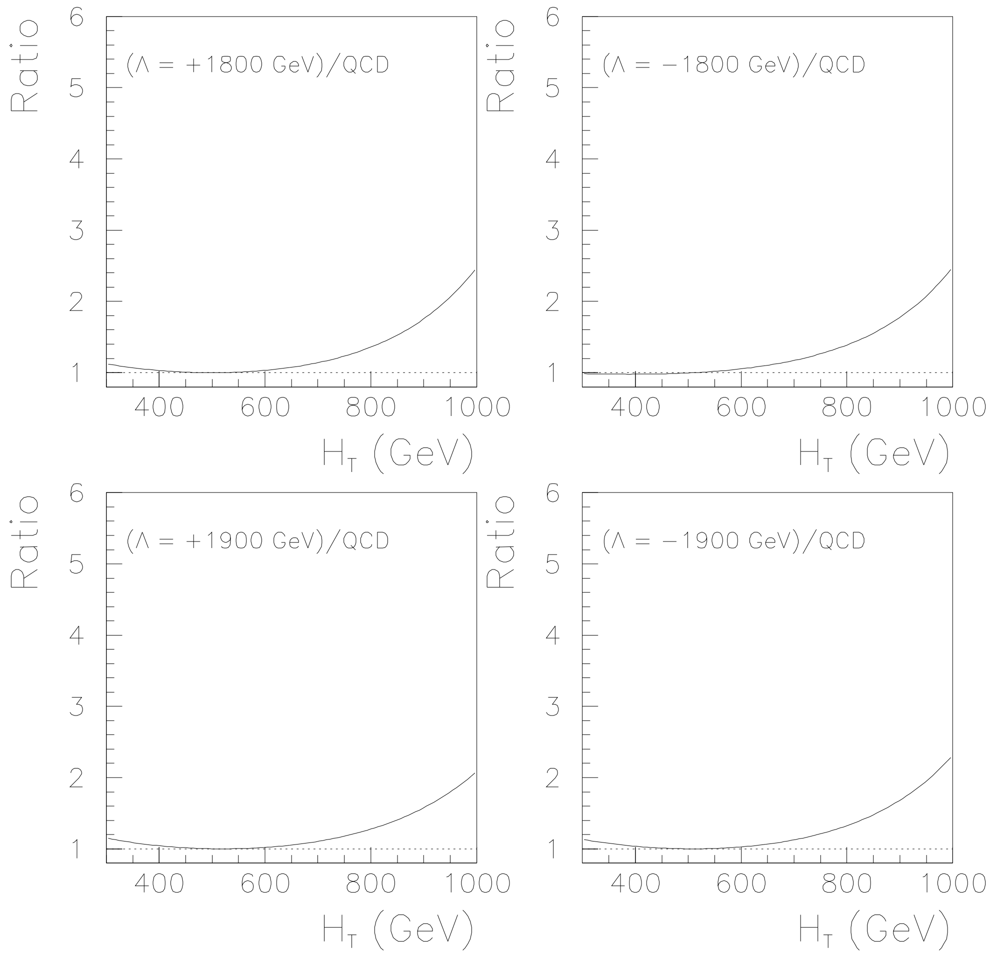

Figure 5: K–factors for $\Lambda = \pm 1800$ and ± 1900 GeV.

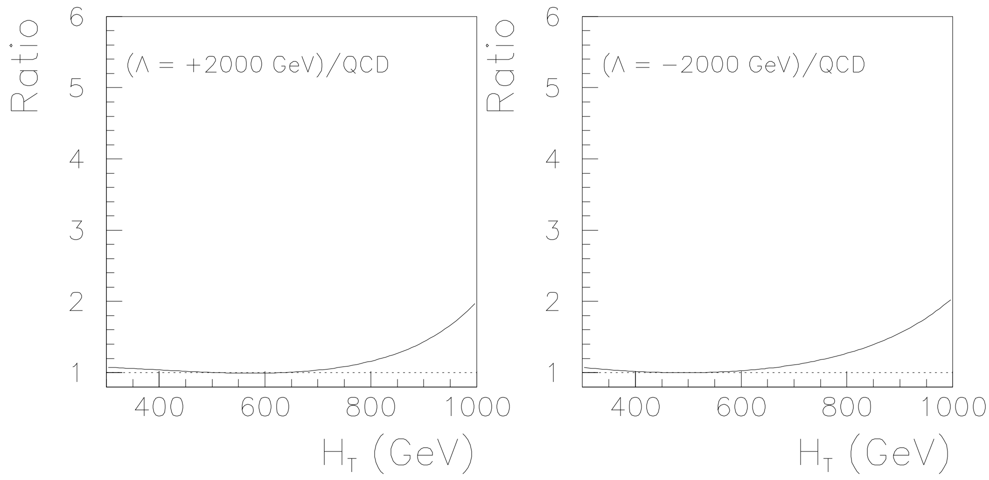

Figure 6: K–factors for $\Lambda = \pm 2000$ GeV.

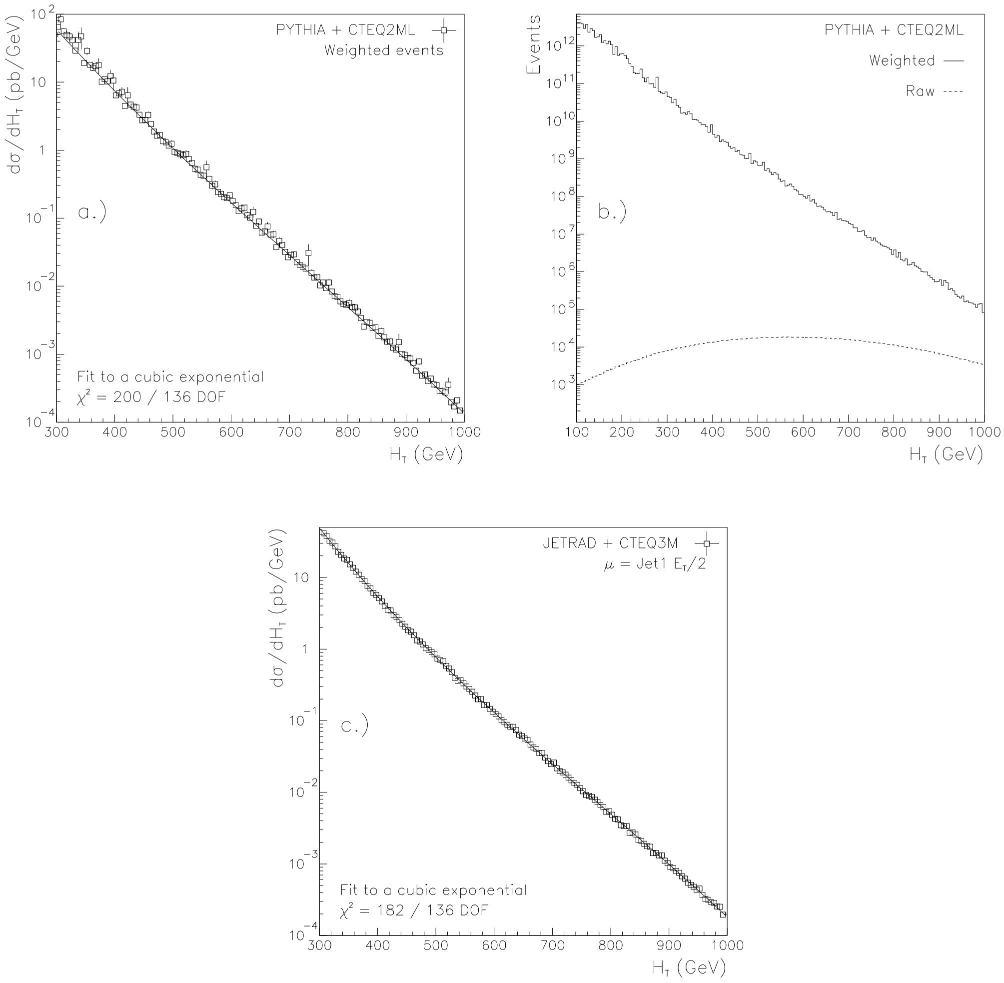

Figure 7: (a)The cross section as a function of H_T generated with PYTHIA. (b)The raw and weighted event distributions generated with PYTHIA using the CTEQ2ML stucture functions and generating 2×10^6 events with the weighting function given in the text. (c)The cross section as a function of H_T generated with JETRAD. The fit to the cubic exponential is described in the text.

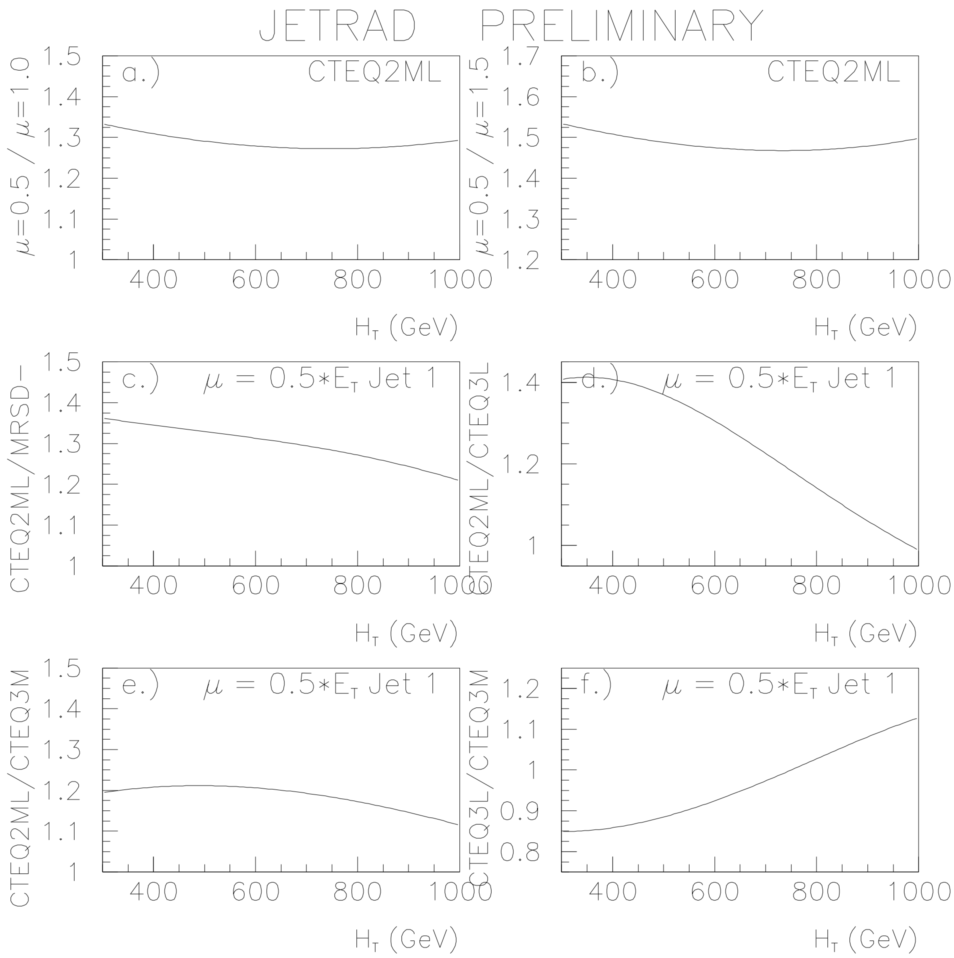

Figure 8: JETRAD study of choice of renormalization scale, μ, and parton distribution function. In (a–b) we show the dependence on the renormalization scale for the CTEQ2ML parton distribution functions. In (c–f) we show the dependence on choice of parton distribution functions for $\mu = 0.5 \times E_T$ of the leading jet.

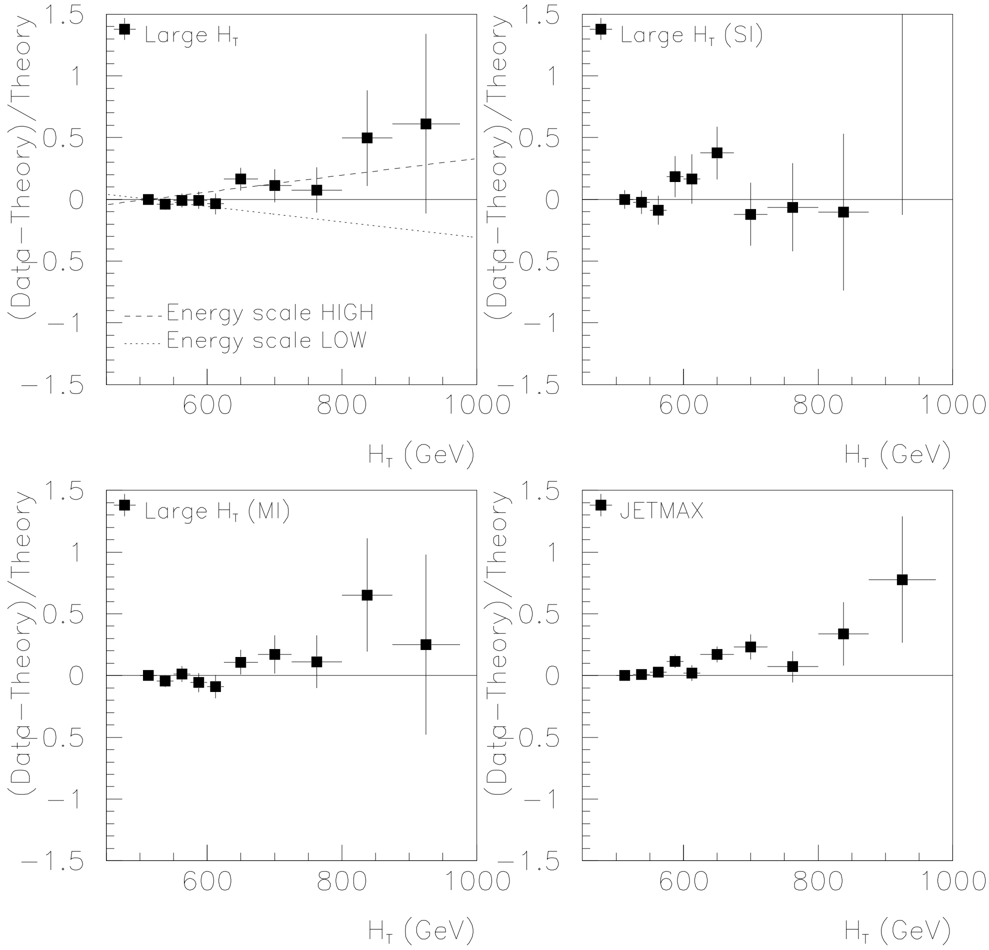

Figure 9: (Data - Theory)/Theory plots for the Large H_T sample (upper left), the Large H_T sample probable single interactions (upper right), the Large H_T sample probable multiple interactions (lower left), and the JETMAX sample (lower right). All comparisons are to JETRAD with the CTEQ3M structure functions and $\mu = 0.5 \times E_T$ of the leading jet.

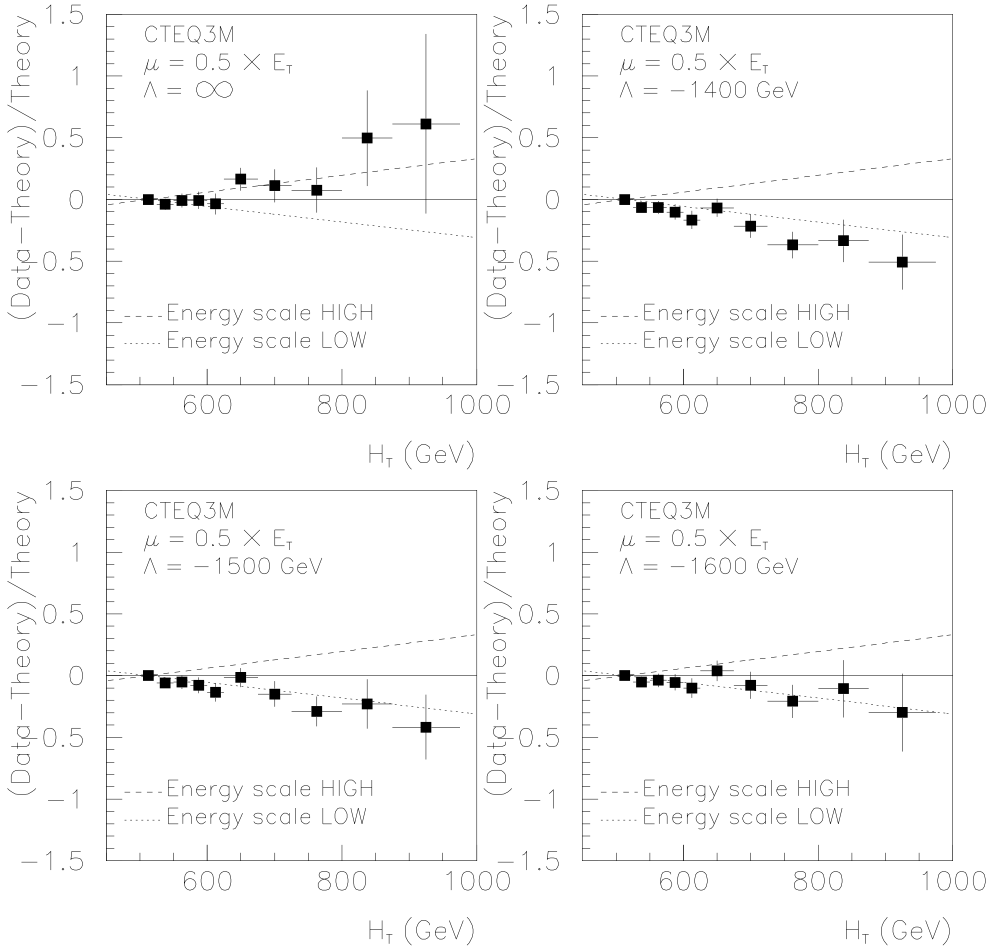

Figure 10: Comparison of Monte Carlo (JETRAD with CTEQ3M and $\mu = 0.5 \times E_T$ of the leading jet) with the Large H_T data sample. Standard model is $\Lambda = \infty$. Included in each plot is the systematic error band due to the jet energy scale uncertainty.

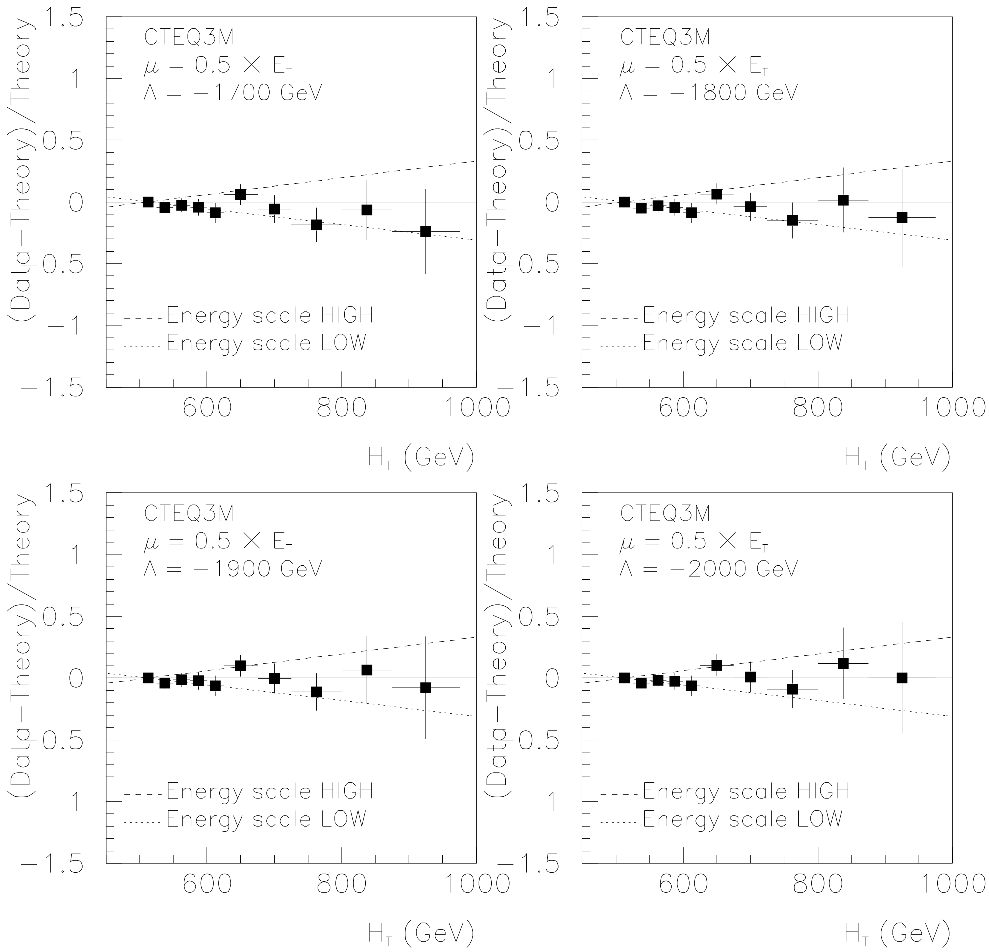

Figure 11: Comparison of Monte Carlo (JETRAD with CTEQ3M and $\mu = 0.5 \times E_T$ of the leading jet) with the Large H_T data sample. Included in each plot is the systematic error band due to the jet energy scale uncertainty.

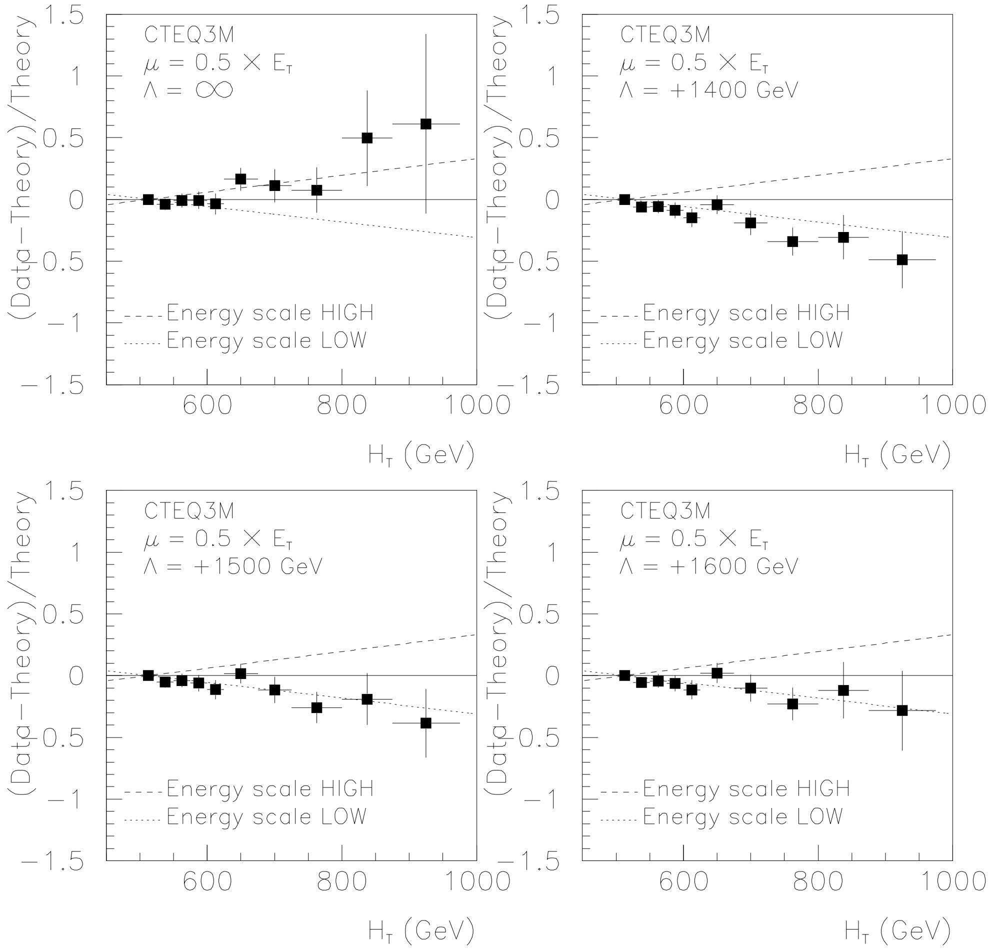

Figure 12: Comparison of Monte Carlo (JETRAD with CTEQ3M and $\mu = 0.5 \times E_T$ of the leading jet) with the Large H_T data sample. Standard model is $\Lambda = \infty$. Included in each plot is the systematic error band due to the jet energy scale uncertainty.

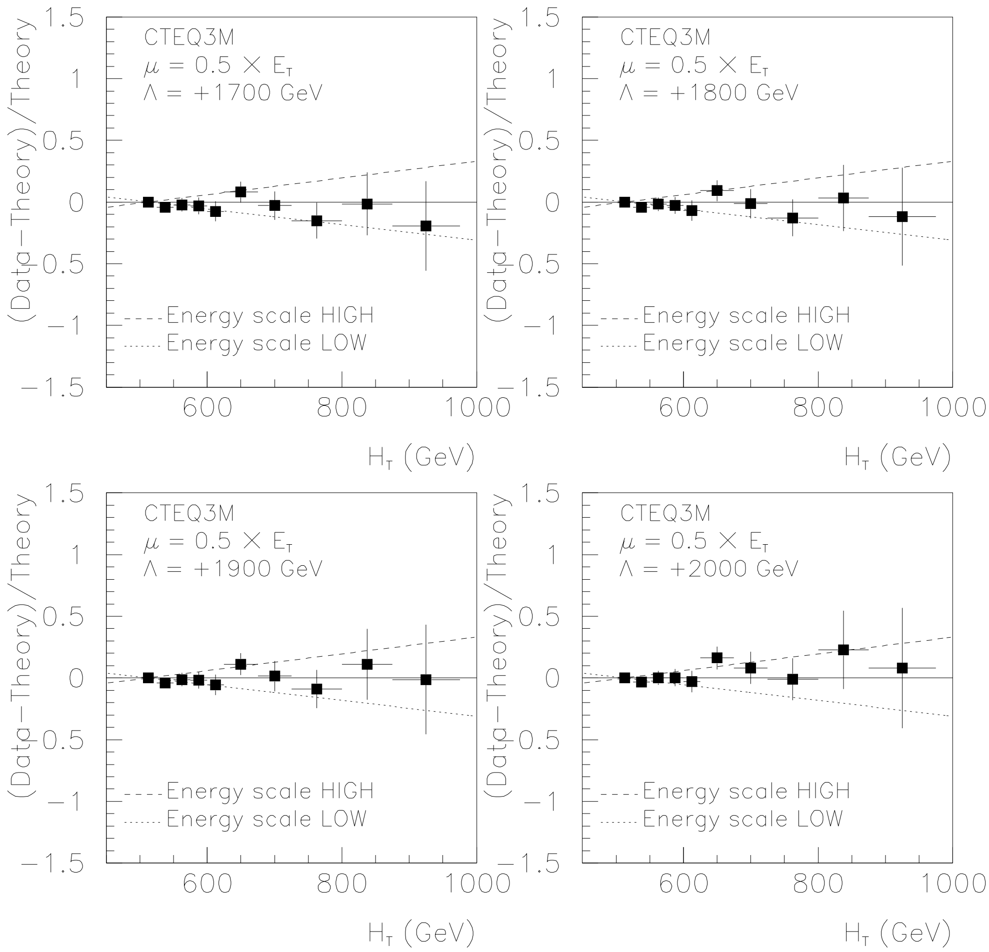

Figure 13: Comparison of Monte Carlo (JETRAD with CTEQ3M and $\mu = 0.5 \times E_T$ of the leading jet) with the Large H_T data sample. Included in each plot is the systematic error band due to the jet energy scale uncertainty.